

# Effect of the Vulcanizing System on the Mechanical Properties of Butyl Rubber/Ethylene Propylene Diene Monomer–Carbon Black Blends

F. Abd-El Salam, M. H. Abd-El Salam, M. T. Mostafa, M. R. Nagy, M. I. Mohamed

Physics Department, Faculty of Education, Ain Shams University, Cairo, Egypt

Received 22 August 2002; accepted 7 January 2003

**ABSTRACT:** The effect of the vulcanizing system on the mechanical properties of butyl rubber/ethylene propylene diene monomer–general purpose furnace black–(GPF) blends was studied with static and dynamic mechanical measurements for these blends. The classical theory of elasticity was applied to show the mechanical behavior of the rubber–polymer blend and to calculate the degree of crosslinking. From the dynamic mechanical measurements,

the elastic modulus, internal friction, and thermal diffusivity were calculated. The observed variations were explained in view of the role played by both the vulcanizing system and the reinforcing carbon black. © 2003 Wiley Periodicals, Inc. *J Appl Polym Sci* 90: 1539–1544, 2003

**Key words:** IIR/EPDM blends; mechanical; vulcanizing system

## INTRODUCTION

Elastomers are generally crosslinked in a random manner, and therefore, it is difficult to identify the principal effects of modification through the mixing of certain components on the mechanical properties. Bhowmick and De<sup>1–3</sup> studied the interplay of the network structure and the polymer–filler interaction, which controls the physical properties of rubber vulcanizates. The types of crosslinks, depend on the class of accelerators and the curing agent used. So, in sulfur-vulcanized rubber, the strength of vulcanizates depends, besides other parameters, on the network structure, which is composed mainly from monosulfide, disulfide, and polysulfide crosslinks. Vulcanizates containing polysulphide crosslinks are generally weaker than those with monosulphide crosslinks.<sup>4</sup> Monosulfide crosslinks are thermally stable, and hence, vulcanizates of this type show relatively small changes on aging. However, polysulfide crosslinks are thermally unstable, and the vulcanizates undergo reversion because the bond energy of the sulfur crosslinks is smaller than that of the hydrocarbon chains.<sup>5</sup> In this work, we studied dependence of the behavior of the mechanical properties of butyl rubber/ethylene propylene diene monomer–general purpose furnace black (IIR/EPDM–GPF) blends on the type of vulcanizing system.

## Materials and techniques

### Materials

All of the concentrations in this work are expressed in parts per hundred rubber by weight (phr). The blend formulation containing IIR (90 phr), EPDM (10 phr), ZnO (5 phr), stearic acid (2 phr), processing oil (10 phr), *N*-cyclohexyl-2-benzthiozyle sulfenamide (1.5 phr), and different contents of GPF black up to 80 phr was vulcanized separately with a constant concentration of 3 phr of one of the following vulcanizing systems: (1) elemental sulfur (S system); (2) tetramethylthiuram disulfide (TMTD); (T system); and (3) elemental sulfur and TMTD; (M system). The prepared compounded rubber was left for at least 48 h before the vulcanization. The vulcanization process was conducted at  $160 \pm 2^\circ\text{C}$  under a pressure of  $40 \text{ kg/cm}^2$  for 20 min.

## Measurements

### Mechanical measurements

*Static mechanical properties (tensile testing).* Dumbbell-shaped samples were cut from the vulcanized sheets by a fine edge steel die with a constant width of 4 mm. The thickness of the test sample was determined with a dial gauge. The apparatus used for stress–strain measurements was a locally manufactured device described elsewhere.<sup>6</sup> The samples were stretched at a constant speed (10 mm/min) that was adjusted by means of direct-current motors. The corresponding force was recorded continuously (each 0.5 min) during the extension until the rupture of the sample. From the

Correspondence to: M. H. Abd-El Salam (mokhtarhemdan@lycos.com).

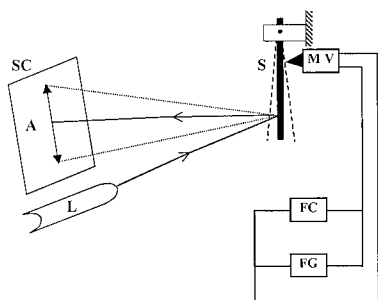


**Figure 1** Schematic diagram for the system of the dynamic resonance technique.

tensile data, the following parameters were calculated as follows:<sup>7</sup>

$$\lambda = L/L_0, \sigma = F/A_0, \epsilon_T = \ln \lambda, \text{ and } \sigma_T = \sigma \lambda \quad (1)$$

where  $\lambda$  is the extension ratio;  $L$ , and  $L_0$  are the lengths of the deformed and nondeformed samples, respectively;  $\sigma$  is the nominal stress;  $F$  is the force;  $A_0$  is the area of the unstrained sample;  $\epsilon_T$  is the true strain; and  $\sigma_T$  is the true stress.

*Dynamic resonance method for the measurement of the dynamic elastic modulus ( $Y_d$ ) internal friction ( $Q^{-1}$ ) and thermal diffusivity ( $D_{th}$ ).*  $Q_w$ ,  $Y_d$ , and  $D_{th}$  measurements were carried out by the application of the dynamic resonance technique, which is based on a standing-wave phenomenon. A measurement similar to that used before<sup>8</sup> is shown in Figure 1. The mechanical electromagnetic vibrator (MV) was derived with a signal from the function generator (FG), whose frequency was indicated by a frequency counter (FC). The sheet under test (S) was clamped at one end and vibrated at the other free end. Its maximum amplitude (A) at the resonance frequency was displayed on a screen (SC) with a laser beam from a low-power laser source (L) reflected from a point at the free vibrating end. The maximum amplitude decreased for lower or higher frequencies than the resonance frequency ( $F_r$ ). From the resonance curve, the full width at half-maximum ( $\Delta F$ ) was obtained. The mechanical parameters  $Q^{-1}$ ,  $D_{th}$ , and  $Y_d$  were obtained as follows:<sup>9</sup>

$$Q^{-1} = \frac{\Delta F}{\sqrt{3}F_0} \quad (2)$$

$$D_{th} = 2d^2F_0/\pi \quad (3)$$

$$Y_d = (2\pi L^2F_0/\kappa Z^2d)^2\rho \quad (4)$$

where  $d$  is the thickness of the sample,  $K$  is the radius of gyration of the cross-section about the axis perpendicular to the plane of vibration, the constant  $Z$  depends on the mode of vibration and equals 1.8751 for

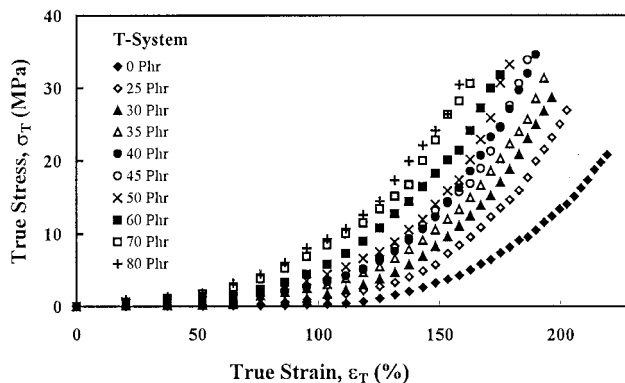


**Figure 2**  $\sigma_T$ - $\epsilon_T$  curves of IIR/EPDM blends loaded with different GPF black contents at room temperature for the T system as a representative example.

the fundamental mode,  $\rho$  is the density of the sample, and  $L$  is the length of the vibrating part of the sample.

## RESULTS AND DISCUSSION

### Static mechanical properties

#### $\sigma_T$ - $\epsilon_T$ strain curves

The  $\sigma_T$ - $\epsilon_T$  curves of IIR/EPDM composites with different vulcanizing systems obtained at room temperature are given in Figure 2 for the T system as a representative example. This figure shows the conventional behavior of the thermosetting materials, where each curve consists of two distinct regions: an initial linear (elastic) region followed by a plastic region. The slope of the initial linear part of any curve in Figure 2 gives Young's modulus ( $Y$ ) which can be taken as a measure for the stiffness of the sample. Figure 3 represents the variation of  $Y$  with carbon black content for different vulcanizing systems. The incorporation of carbon black into the IIR/EPDM rubber matrix increased  $Y$ . In vulcanized rubber, the strength of vulcanizates depends, besides other parameters, on the

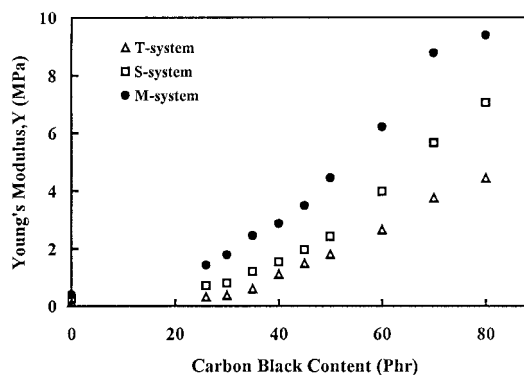


**Figure 3** Variation of  $Y$  with carbon black content for different vulcanizing systems.

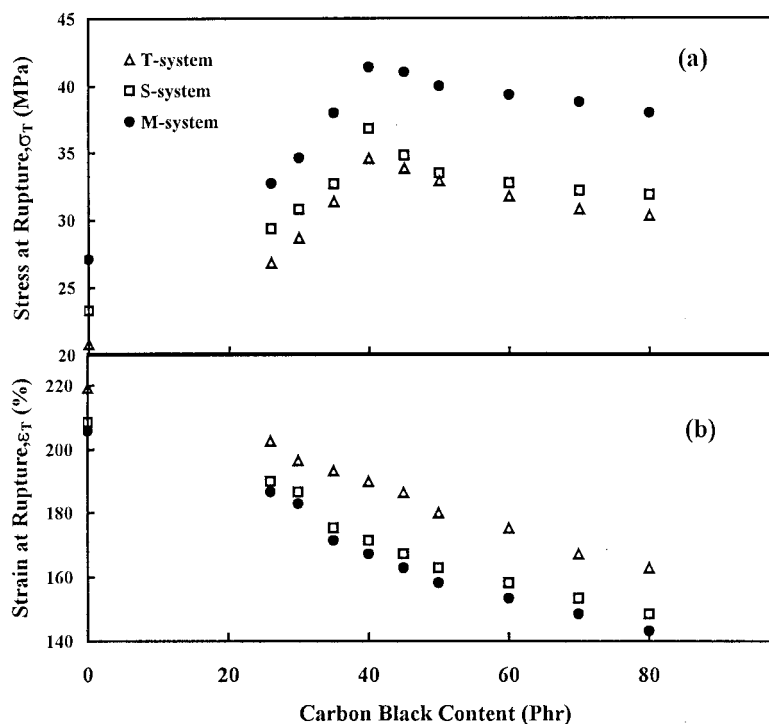


Figure 4 Dependence of  $\sigma_f$  and  $\epsilon_f$  on the carbon black content for different vulcanizing systems.

concentration of added filler and the type of the existing crosslinks, which mainly depend on the curing agent used.<sup>10</sup> The values of  $Y$  for the M system were higher than those of the S and T systems. This might have been due to the different types of crosslinks<sup>11</sup> resulting from these systems. It was assumed that the T vulcanizing system created in the rubber vulcanizates crosslinks of the monosulfide and disulfide ( $-S-$  and  $-S-S-$  respectively) types, whereas the S and M systems created mixed crosslinks of the monosulfide, disulfide, and polysulfide types but in different ratios. Vulcanizates containing polysulfide crosslinks were generally found to be considerably weaker than those with monosulfide ( $-S-$ ).<sup>10</sup> So, the crosslinking of IIR/EPDM composites was more affected by the mixed system S + TMTD than by either S or TMTD. Figure 4 shows the dependence of the stress at rupture ( $\sigma_f$ ) and the strain at rupture ( $\epsilon_f$ ) on carbon black content. Generally, for the three composites,  $\sigma_f$  increased with increasing carbon black content, showing maxima around 40 phr GPF black, followed by a decrease with further increases of the content of GPF black. This behavior suggested the formation of a compact structure, and above a content of 40 phr GPF, this compact structure became more loose.<sup>12</sup> The values of  $\sigma_f$  for the M system were higher than those of both the S and T systems. This may have been due to the state of the crosslinks in the case of M system, which were more effective than both the S and T systems. As shown in Figure 4(b),  $\epsilon_f$  decreased with increasing carbon black content. This might have been

due to the formation of carbon black aggregates between the flexible chain segments, which acted as obstacles to their sliding. It is also clear from Figure 4(b) that the TMTD-cured IIR/EPDM showed higher levels for the strain at break than those of the S and M systems. Therefore, we concluded that TMTD-cured IIR/EPDM showed superior performance to the two other vulcanizing systems used.

#### Determination of the degree of crosslinking

The classical theory of elasticity<sup>13</sup> is described by the following expression:

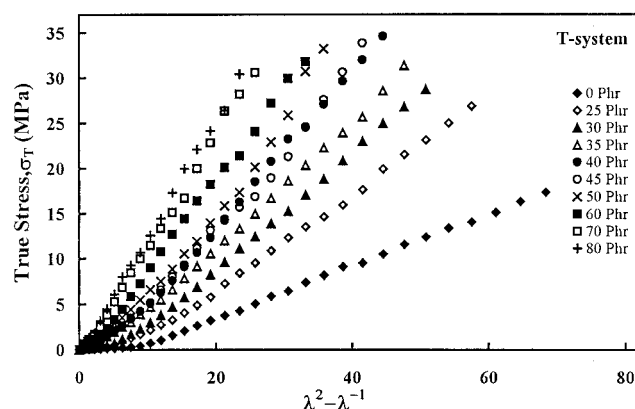


Figure 5 Dependence of  $\sigma_T$  on  $\lambda^2 - \lambda^{-1}$  for IIR/EPDM blends loaded with different GPF black contents at room temperature for the T system as a representative example.

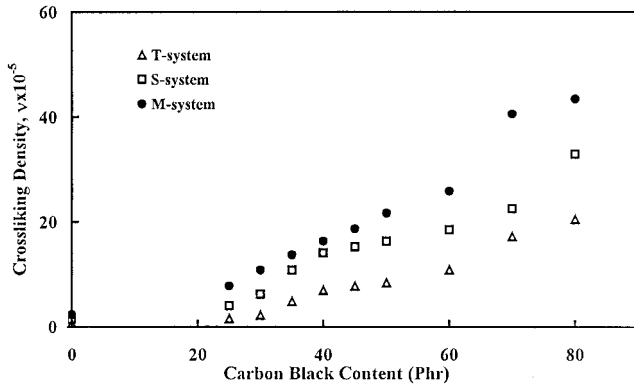


Figure 6 Variation of  $v$  with carbon black content for different vulcanizing systems.

$$\sigma_T = \sigma_0 + G(\lambda^2 - \lambda^{-1}) \quad (5)$$

where  $\sigma_0$  is the steady-state component of  $\sigma_T$ , which depends on the chemical nature of the rubber, and  $G$  is the rubbery modulus, which depends on  $v$ . The dependence of  $\sigma_T$  on  $\lambda^2 - \lambda^{-1}$  for samples of different

vulcanizing systems are represented by the data of the T system given in Figure 5. The slope of the initial linear part of any of these curves gave  $G$ .  $G$  depended on both the carbon black content and the vulcanizing system. The M system had higher  $G$  values than the S and T systems. From the obtained values of  $G$ , the average molecular mass between two crosslinks ( $M$ ) was calculated with the following relation:<sup>14</sup>

$$M_c = \frac{\rho RT}{G} \quad (6)$$

where  $\rho$  is the density of rubber,  $R$  is the gas constant, and  $T$  is the absolute temperature. (g mol of crosslinks/unit g of rubber) was calculated with eq. (6) in the following relation:

$$v = 1/(2M_c) \quad (7)$$

Figure 6 shows the variation of  $v$  with increasing carbon black content.  $v$  increased with increasing carbon

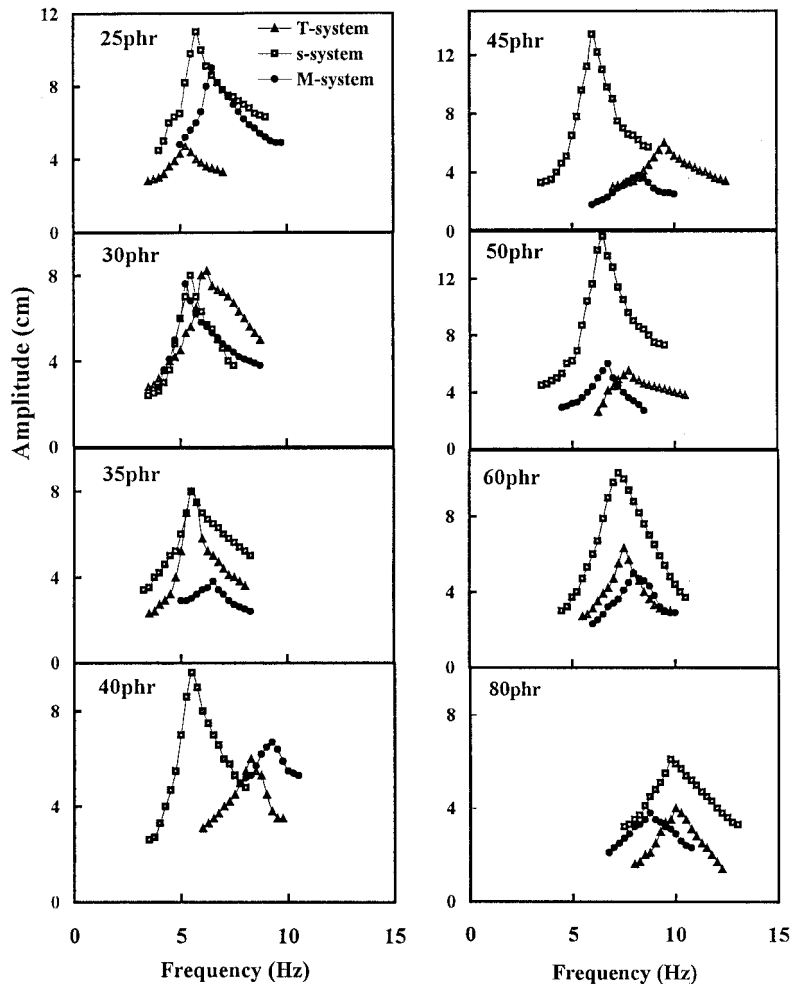


Figure 7 Resonance curves of IIR/EPDM blends loaded with different GPF carbon black contents for vulcanizing systems (▲) T, (■) S, and (●) M.

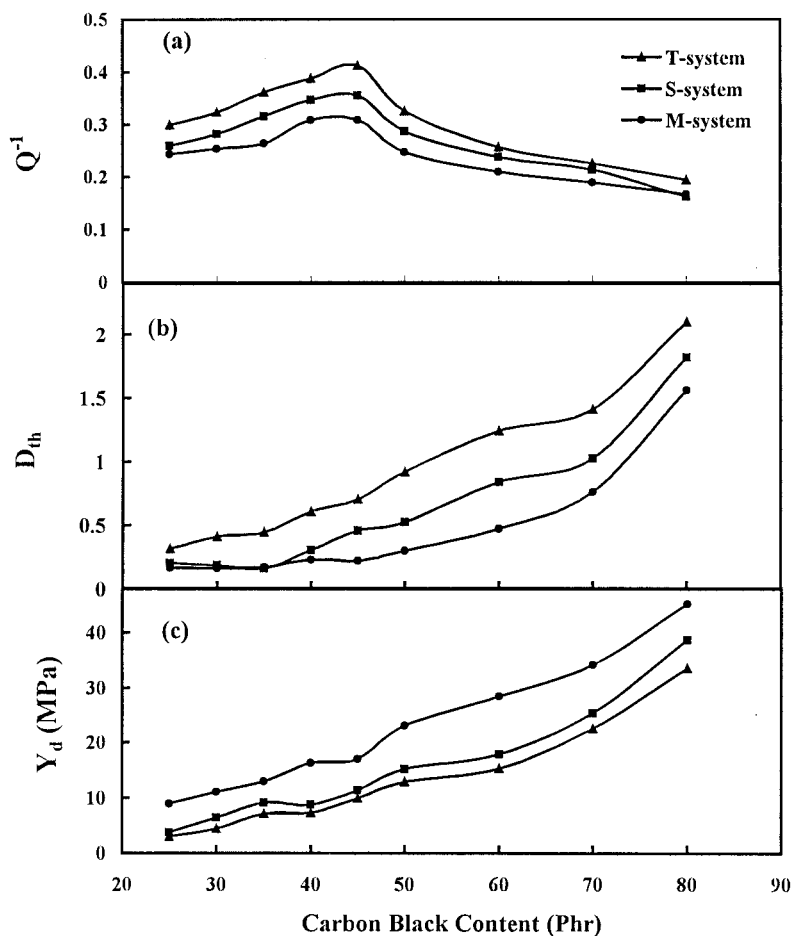


Figure 8 Dependence of (a)  $Q^{-1}$ , (b)  $D_{th}$ , and (c)  $Y_d$  on the carbon black content for vulcanizing systems (▲) T, (■) S, and (●) M.

black content. The role of carbon black to create crosslinks was effective all over the concentration range for the M system, whereas for both the S and T systems, it seemed to be more difficult, as was clear from their lower levels of  $\nu$ , as shown in Figure 6.

### Dynamic mechanical properties

Rubber friction differs in many ways from the frictional properties of most other solids. The reason is the very low  $Y_d$  and the high  $Q^{-1}$  exhibited by rubber in a wide frequency region.<sup>15</sup> Dynamic mechanical testing, in general, gives more information about a tested polymer than static testing because of its high sensitivity to the chemical and physical structures of a polymer. The resonance curves of the tested samples with different carbon black contents are given in Figure 7. From Figure 7, the values of  $Q^{-1}$  (taken as the ratio of energy dissipated as heat to the maximum energy stored in the material during one cycle),  $D_{th}$ , and the  $Y_d$  are given as function of carbon black content in Figure 8.  $Q^{-1}$  values for all of the tested samples [Fig. 8(a)] generally increased with increasing

carbon black content, showing maxima around 40 phr GPF carbon black, followed by a decrease with further increases in GPF carbon black content. The maximum vibrating driving force at the resonance frequency enhanced the  $D_{th}$  of carbon particles in the matrix [Fig. 8(b)], and the dispersion of these particles led to the creation of crosslinks that brought the polymer chain segments to a more stable state and increased the strength of the sample, as is clear in Figure 8(c). The low  $\nu$  created with low carbon content [Fig. (6)] increased the number of the isolated stabilized chain segments and increased the friction generated at the interfacial crosslink-free areas adjacent to the stabilized crosslinked segments. Also, the nonresonant bowing of the crosslink-free chain segments represented in itself some hysteretic  $Q^{-1}$ ,<sup>16</sup> such that a maximum for  $Q^{-1}$  was reached at 40 phr GPF black. Further increases in carbon content above 40 phr led to increased  $\nu$ . The stabilized segments, which became less in number and greater in size due to the high diffusivity of carbon atoms, reduced the chain movements, and therefore,  $Q^{-1}$  decreased with increasing carbon content. It was, therefore, the  $\nu$  that controlled

the levels of the parameters  $Q^{-1}$ ,  $D_{thv}$ , and  $Y_d$  in relation to carbon content.<sup>17</sup> From the maxima observed in Figures 4 and 8, it was clear that these data covered a wide range of variation with opposite behavior and different levels for the values of the mechanical properties. In general, the data show that the vulcanizing system controlled the level of the measured parameters but that the carbon black content modified the dynamic properties of the rubber endproduct. Hence, the proper selection of the vulcanizing system and carbon black type and content is necessary for optimum performance, especially, for example, in applications where the controlled damping of mechanical vibrations is essential.

### CONCLUSION

The effect of vulcanizing system on the mechanical properties of IIR/EPDM blends reinforced with GPF carbon black was studied. The tensile strength and  $Y$  were enhanced by the addition of carbon black (Figs. 3 and 4). The level of  $\nu$  was higher for the M vulcanizing system than for both the S and T systems. This was taken as a base to discuss the variations observed for the mechanical properties. Measurements of  $Q^{-1}$ ,  $D_{thv}$ , and  $Y_d$  obtained for the different composites revealed the effect of carbon black content and the role of  $\nu$  on the observed variations of the data obtained for the different investigated systems. The proper se-

lection of the vulcanizing system and the type and content of carbon black is necessary for optimum performance of the rubber endproduct.

### References

1. Bhowmick, A. K.; De, S. K. *J Appl Polym Sci*, 1980, 26, 529.
2. Bhowmick, A. K.; De, S. K. *Rubber Chem Technol* 1980, 53, 960 and 1015.
3. Bhowmick, A. K.; De, S. K. *Rubber Chem Technol* 1979, 52, 985.
4. Kim, S. G.; Lee, S. H. *Rubber Chem Technol* 1994, 67, 649.
5. Hoffman, W. *Vulcanization and Vulcanizing Agents*; Farbenfabriken Bayer AG: Lever Kusen, Germany; pp 17, 80, 92, 98, and 104.
6. Abd El-Salam, M. H. Ph.D. Thesis, Cairo University, 1977; p 41.
7. Kaufman, H. S. *Introduction to Polymer and Technology*; An SPE Textbook; Wiley-Interscience: New York, 1970.
8. Abd El-Salam, F.; Mostafa, M. T.; Nada, R. H.; Abd El-Khalek, A. M. *Phys Status Solidi A* 2001, 185, 331.
9. Spineer, S.; Teffit, W. E. *Am Soc Test Mater Proc* 1961, 61, 1221.
10. El-Sabbagh, S. H.; Ismail, M. N.; Yehia, A. A. *J Elastomers and Plastics* 2001, 33, 263.
11. Morrison, N. J.; Porter, M. *Rubber Chem Technol* 1983, 57, 63.
12. Eatah, A. I.; Ghani, A. A.; Hashem, A. A. *Polym Degrad Stab* 1990, 27, 75.
13. Zang, Y. H.; Muller, R.; Froelich, D. *Soc Rheol*. 1986, 30, 1165.
14. Blow, C. M. *Rubber Technology and Manufacture*; Institute of Rubber Industry; London, 1971.
15. Persson, B. N. J. *Surf Sci* 1998, 40, 445.
16. Abd El-Salam, F.; Mostafa, M. T.; Nada, R. H.; Abd El-Khalek, A. M. *Phys Status Solidi* 2001, 185, 331.
17. Murayama, T.; Bell, J. P.; *J Polym Sci Part A-2 Polym Phys* 1970, 8, 437.